

# LONG RANGE BEAM-BEAM EFFECTS IN THE LHC

W. Herr, X. Buffat, R. Calaga, R. Giachino, G. Papotti, T. Pieloni,  
D. Kaltchev (TRIUMF, Vancouver, Canada)

## Abstract

We report on the observations of long range beam-beam effects during dedicated studies as well as the experience from operation. Where possible, we compare the observations with the expectations.

## LAYOUT FOR BEAM-BEAM INTERACTIONS

The layout of experimental regions in the LHC is shown in Fig.1. The beams travel in separate vacuum chambers

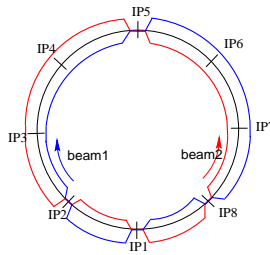


Figure 1: Layout of the experimental collision points in the LHC [1, 2].

and cross in the experimental areas where they share a common beam pipe. In these common regions the beams experience head-on collisions as well as a large number of long range beam-beam encounters [1, 2, 3]. This arrangement together with the bunch filling scheme of the LHC as shown in Fig.2 [1, 3] leads to very different collision pattern for different bunches, often referred to as "PAC-MAN" bunches. The number of both, head-on as well as

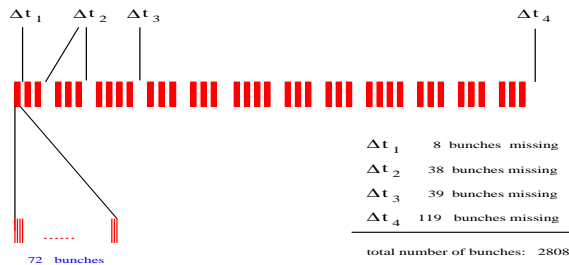


Figure 2: Bunch filling scheme of the nominal LHC.

long range encounters, can be very different for different bunches in the bunch trains and lead to a different integrated beam-beam effect [2, 3]. This was always a worry in the LHC design and the effects have been observed in an early stage of the commissioning. Strategies have been

provided to minimize these effect, e.g. different planes for the crossing angles [1, 3].

## Strength of long range interactions

A key parameters for the effect of long range interactions is the local beam separation at the parasitic encounters. Usually this separation is measured in units of the transverse beam size at the corresponding encounter. As standard and for comparison between different configurations, we use the normalized separation in the drift space. For small enough  $\beta^*$  and round beams it can be written as a simple expression:

$$d_{sep} \approx \frac{\sqrt{\beta^*} \cdot \alpha \cdot \sqrt{\gamma}}{\sqrt{\epsilon_n}}$$

Beyond the drift space the exact separation has to be computed with an optics program. For a small  $\beta^*$  the phase advance varies fast between the head-on interaction point and the first parasitic encounter from 0 to  $\frac{\pi}{2}$ . Most of the parasitic encounters occur at similar phases and therefore can add up. This is in strong contrast to other separation schemes such as pretzl separation used in the SPS collider and the Tevatron, where the parasitic encounters are distributed around the whole ring. The separation is easier to control in the case of a crossing angle than for a global separation. A strong, local non-linearity can be expected to have a strong effect, but opens the possibility of a correction. Possible correction schemes are discussed in a dedicated session at this workshop [4].

## STUDIES OF LONG RANGE INTERACTIONS

Contrary to the head-on beam-beam effects, the long range beam-beam interactions is expected to play an important role for the LHC performance and the choice of the parameters [5, 6]. To study the effect of long range beam-beam interactions we have performed two dedicated experiments. In the first experiment, the LHC was set up with single trains of 36 bunches per beam, spaced by 50 ns. The bunch intensities were  $\approx 1.2 \cdot 10^{11}$  protons and the normalized emittances around  $2.5 \mu\text{m}$ . The trains collided in IP1 and IP5, leading to a maximum of 16 long range encounters per interaction point for nominal bunches. First, the crossing angle (vertical plane) in IP1 was decreased in small steps and the losses of each bunch recorded. The details of this procedure are described in [7]. In the second experiment we injected 3 trains per beam, with 36 bunches per train. The filling scheme was chosen

such that some trains have collisions in IP1 and IP5 and other collide only in IP2 or IP8.

### Losses due to long-range interactions

From simulations [8] we expected a reduction of the dynamic aperture due to the long-range beam-beam encounters and therefore increased losses when the separation is decreased. To estimate the losses, we have shown in Fig.3

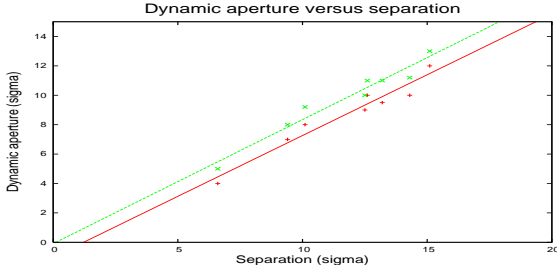


Figure 3: Expected dynamic aperture as function of separation in drift space [8]. Computed for 50 ns and 25 ns separation.

the expected dynamic aperture as a function of the normalized separation [8] for two different bunch spacings (50 ns and 25 ns). The separation was varied by changing the crossing angle as well as the  $\beta^*$ . From this figure we can determine that visible (i.e. recordable) we can expect for a dynamic aperture around  $3\sigma$  and therefore when the separation is reduced to values around  $5\sigma$ . For larger separation the dynamic aperture is also decreased but the losses cannot be observed in our experiment.

### Losses due to long range encounter during operation

Significant losses have also been observed during regular operation. Given that the expected dynamic aperture is closely related to the normalized separation as shown in Fig.3, this separation should be kept large enough and if possible constant during an operation of the machine. From the expression for the normalized separation it is clear that a change of  $\beta^*$  requires a change of the crossing angle  $\alpha$  to keep the separation constant.

For the first attempt to squeeze the optical functions from  $\beta^* = 1.5$  m to  $\beta^* = 1.0$  m, the crossing angle was decreased to reduce the required aperture, thus reducing the separation at the encounters. During the ramp, an instability occurred which (probably) increased the emittances of all bunches, reducing further the normalized beam separation. When the optics was changed, very significant beam losses occurred (see Fig.4) for those bunches colliding in interaction points 1 and 5, where the separation was reduced due to smaller  $\beta^*$ . Bunches colliding only in interaction points 2 and 8 are not affected. This clearly demonstrates the strong effect of long range encounter and the need for sufficient separation.

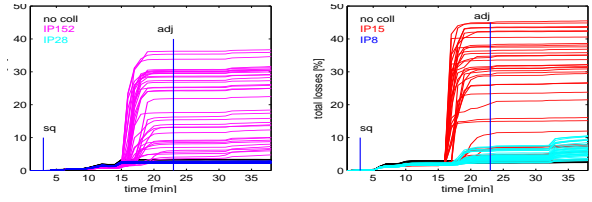


Figure 4: Losses in beam 1 and beam 2 with too small separation.

### Losses due to long range encounter during dedicated experiment

We have performed two measurements and the results of the first experiment are shown in Fig.5 where the integrated losses for the 36 bunches in beam 1 are shown as a function of time and the relative change of the crossing angle is given in percentage of the nominal ( $100\% \equiv 240 \mu\text{rad}$ ). The nominal value corresponds to a separation of approximately  $12\sigma$  at the parasitic encounters.

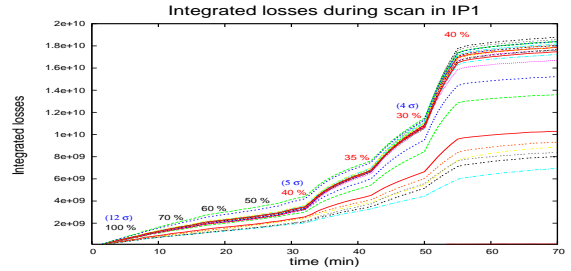


Figure 5: Integrated losses of all bunches as a function of time during scan of beam separation in IP1. Numbers show percentage of full crossing angle.

The losses per bunch observed in the second experiment are shown in Fig.6. The observed behaviour is very similar. In this experiment we have set up several trains with differ-

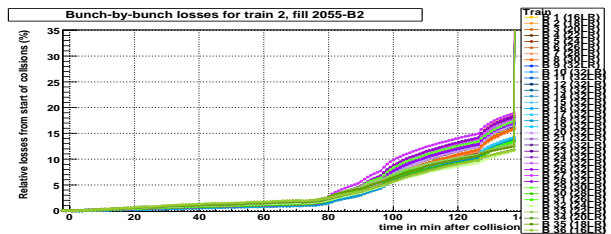


Figure 6: Integrated losses of bunches as a function of time during scan of beam separation in IP1. Bunches colliding in IP1 and IP5. Numbers show percentage of full crossing angle.

ent collision schemes and in Fig.7 we show the losses in the bunches colliding in IP8, but not in IP1 and IP5 where the separation was reduced. As expected, this reduction had no effect on the losses of these bunches (please note change of

the scale). In Fig.8 we show the vertical emittances for all

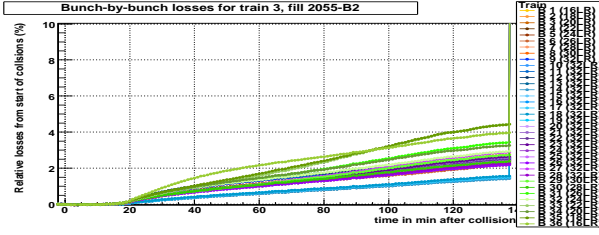


Figure 7: Integrated losses of bunches as a function of time during scan of beam separation in IP1. Bunches without collisions in IP1 and IP5. Numbers show percentage of full crossing angle.

bunches during this second experiment. Such a measurement was not available in the first study. From Figs.5 and 6

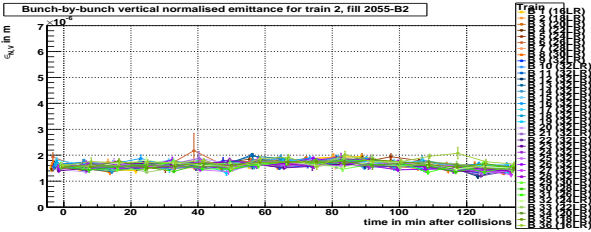


Figure 8: Vertical emittances all bunches as a function of time during scan of beam separation in IP1.

we observe significantly increased losses for some bunches when the separation is reduced to about 40%, i.e. around  $5\sigma$ . The emittances are not affected by the reduced separation (Fig.8) and we interpret this as a reduction of the dynamic aperture as expected from the theory and simulations. The emittances, mainly determined by the core of the beam, are not affected in this case.

### Bunch to bunch differences and PACMAN effects

Not all bunches are equally affected. At a smaller separation of 30% all bunches experience significant losses ( $\approx 4\sigma$ ). Returning to a separation of 40% reduces the losses significantly, suggesting that mainly particles at large amplitudes have been lost during the scan due to a reduced dynamic aperture. Such a behaviour is expected [9, 8]. The different behaviour is interpreted as a "PACMAN" effect and should depend on the number of long range encounters, which varies along the train. This is demonstrated in Fig.9 where we show the integrated losses for the 36 bunches in the train at the end of the experiment. The maximum loss is clearly observed for the bunches in the centre of the train with the maximum number of long range interactions (16) and the losses decrease as the number of parasitic encounters decrease. The smallest loss is found for bunches with the minimum number of interactions, i.e. bunches at the beginning and end of the train [1, 3]. It is demonstrated in Fig.10 where we shows the integrated losses and in the

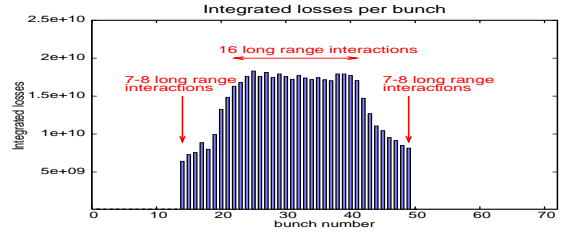


Figure 9: Integrated losses of all bunches along a train of 36 bunches, after reducing the crossing angle in IP1.

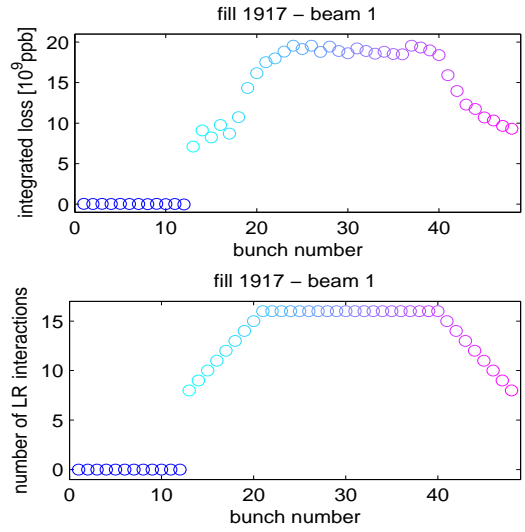


Figure 10: Integrated losses of all bunches along a train of 36 bunches, after reducing the crossing angle in IP1. Second figure shows number of long range encounters for the same bunches.

second figure for the same bunches the number of long range encounters. The agreement is rather obvious. This is a very clear demonstration of the expected different behaviour, depending on the number of interactions.

In the second part of the experiment we kept the separation at 40% in IP1 and started to reduce the crossing angle in the collision point IP5, opposite in azimuth to IP1 (Fig.1). Due to this geometry, the same pairs of bunches meet at the interaction points, but the long range separation is in the orthogonal plane. This alternating crossing scheme was designed to compensate first order effects from long range interactions [1]. Fig.11 shows the evolution of the luminosity in IP1 as we performed the scan in IP5. The numbers indicate again the relative change of separation, this time the horizontal crossing angle in IP5. The luminosity seems to show that the lifetime is best when the separation and crossing angles are equal for the two collision points. It is worse for smaller as well as for larger separation. This is the expected behaviour for a passive compensation due to alternating crossing planes, although further studies are required to conclude. A more quantitative comparison with the expectations is shown in Fig.12. The dynamic aperture in units of the beam size is shown as a function of the beam

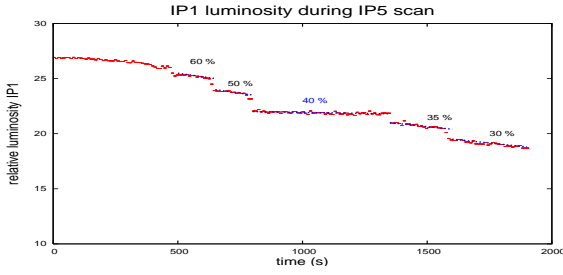


Figure 11: Luminosity in IP1 as a function of time during scan of beam separation in IP5.

separation [8]. From the relative losses in the experimen-

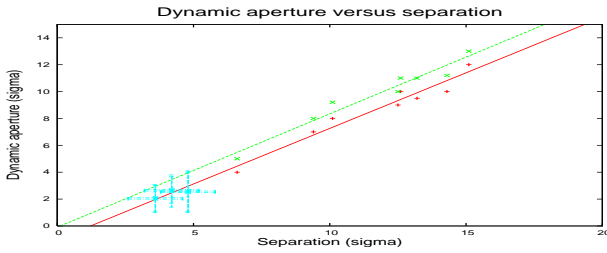


Figure 12: Dynamic aperture versus separation. Comparison with results from experiment.

tal studies, we have tried to estimate the dynamic aperture, assuming a Gaussian beam profile and tails. This measurement can obviously only give a rough estimate, but is in very good agreement with the expectations. At larger separation, the losses are too small to get a reasonable estimate. More information can be obtained from an analytical model [10, 11].

### Further observations of PACMAN effects

The behaviour of so-called PACMAN bunches [3, 12] was always a concern in the design of the LHC. In order to avoid a tune shift of PACMAN bunches relative to the nominal bunches, an alternating crossing scheme was implemented in the LHC [3]. The effect of the alternating crossing scheme on the tune along a bunch train is shown in Fig.13. The computation is based on a self-consistent calculation of orbits and all optical beam parameters [13]. Without the alternating crossing, the PACMAN bunches

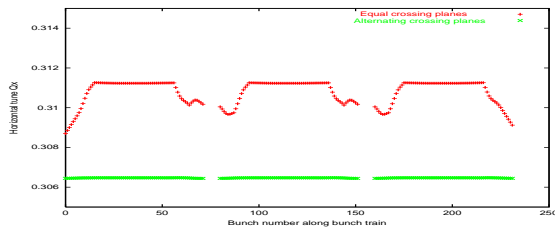


Figure 13: Computed tune along bunch train for equal and alternating crossing planes [1, 3].

exhibit a strong dependence of their tunes on their posi-

tion in the bunch train. Depending on the intensity, bunch spacing and separation, this spread can exceed  $2 \cdot 10^{-3}$ . The alternating crossing scheme compensates completely for this spread. This compensation is incomplete when bunch to bunch fluctuations are taken into account, but in all cases the compensation is efficient [3]. This compensation is largely helped by the design feature that the two low  $\beta^*$  experimental regions are exactly opposite in azimuth (see Fig.1) [2] and the same bunch pair collide in the two regions with alternating crossings and the same optical parameters. This requires that the contribution to the long range beam-beam effects from the other two experiments is small. Due to the larger  $\beta^*$  this is guaranteed under nominal operational conditions.

Another predicted behaviour of PACMAN bunches are the different orbits due to the long range interactions. The decreased separation, corresponding to stronger dipolar kicks, clearly lead to orbit changes along the corresponding bunch train. The bunches not participating in collisions in IP1 and IP5 are not affected. To study these effects, a fully self-consistent treatment was developed to compute the orbits and tunes for all bunches in the machine under the influence of the strong long range beam-beam interactions [13]. The Fig.14 show the vertical orbit offsets at IP1 for the two beams in the case of vertical crossings in IP1 and IP5. The figures show a significant effect at the interaction

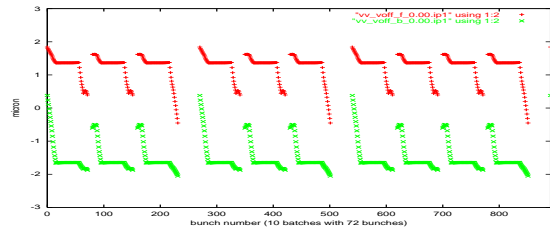


Figure 14: Computed orbit offsets in IP1 for beam 1 and beam 2 two vertical crossings [1, 3, 13].

point and moving the beams it is not possible to make all bunches overlap. The effect of alternating crossings (verti-

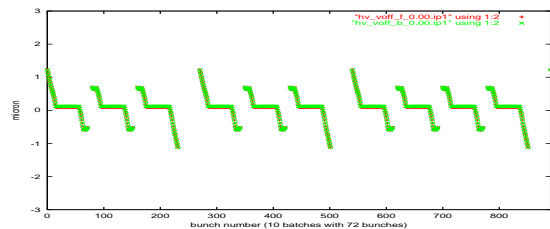


Figure 15: Computed orbit offsets in IP1 for beam 1 and beam 2 alternating crossings [1, 3, 13].

cal in IP1 and horizontal in IP5) is shown in Fig.15. Now the bunches from the two beams can be made overlap exactly, although not at the central collision point. In the other plane this complete overlap cannot be obtained, although the offset is small. In Fig.16 we show a prediction

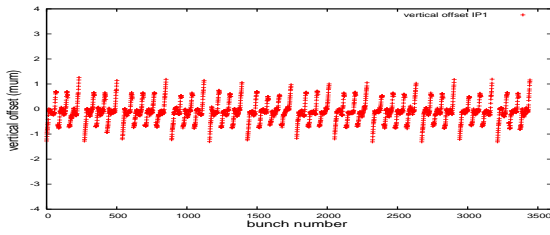


Figure 16: Computed orbit offsets in IP1 along the bunch train [1, 3].

for the vertical offsets in IP1 [1, 3]. The offsets should vary along the bunch train. Although the orbit measurement in the LHC is not able to resolve these effects, the vertex centroid can be measured bunch by bunch in the experiment. The measured orbit in IP1 (ATLAS experiment) is shown

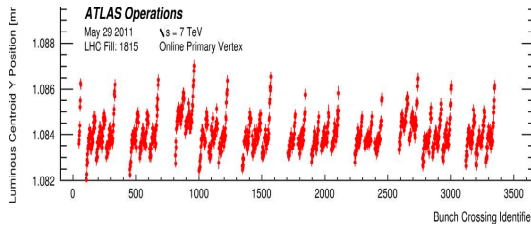


Figure 17: Measured orbit offsets in IP1 along the bunch train [14, 15].

in Fig.17 and at least the qualitative agreement is excellent. This is a further strong indication that the expected PACMAN effects are present and understood and that our computations are reliable.

## PARAMETRIC DEPENDENCE OF LONG RANGE LOSSES

In order to study the dependence of long range effects on the parameters of the beam-beam interaction, we have performed the experiments with different parameters, in particular different  $\beta^*$  and intensities. The relevant parameters of the three experiments are found in Tab.1. The experi-

experiment	emittance	$\beta^*$	Intensity
2011 (50 ns)	2.0 - 2.5 $\mu\text{m}$	1.5 m	$1.2 \cdot 10^{11}$
2012 (50 ns)	2.0 - 2.5 $\mu\text{m}$	0.6 m	$1.2 \cdot 10^{11}$
2012 (50 ns)	2.0 - 2.5 $\mu\text{m}$	0.6 m	$1.6 \cdot 10^{11}$

Table 1: Parameters for three long range experiments

mental procedure was the same as before: the separation (crossing angle) was reduced until visible losses were observed. The results of a first separation scan are shown in Fig.18. The main observations are:

- Recent test (2012) with  $\beta^* = 0.60\text{m}$ , intensity:  $1.6 \cdot 10^{11}$  p/b

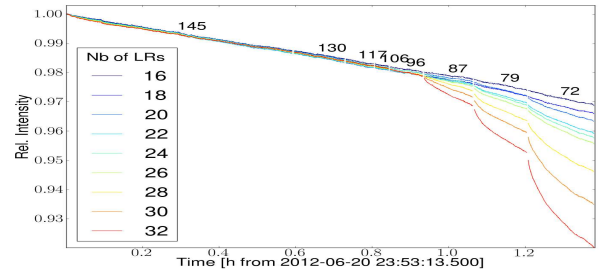


Figure 18: Separation scan with high intensity.

- Initial separation  $\approx 9 - 9.5 \sigma$
- Losses start  $\approx 6 \sigma$  separation

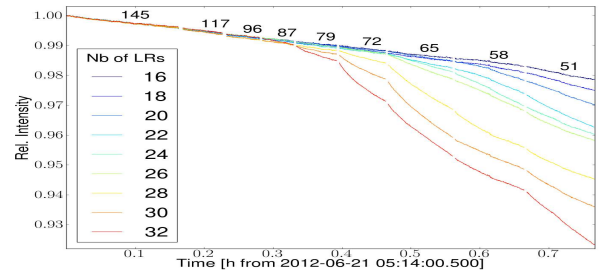


Figure 19: Separation scan with reduced intensity.

The results of a second separation scan are shown in Fig.19. The main observations are:

- Recent test (2012) with  $\beta^* = 0.60\text{m}$ , intensity:  $1.2 \cdot 10^{11}$  p/b
- Initial separation  $\approx 9 - 9.5 \sigma$
- Losses start  $\approx 5 \sigma$  separation

The experiments summarized in Tab.1 have been analysed using a recently developed technique to parametrize the strength of the long range non-linearity, based on the evaluation of the invariant and the smear [10, 11].

This method is applied to compare different configurations [11] and allows to derive scaling laws for the dynamic aperture.

## SUMMARY

We have reported on the first studies of beam-beam effects in the LHC with high intensity, high brightness beams and can summarize the results as:

- Effect of the beam-beam interaction on the beam dynamics clearly established
- Effect of long range interactions on the beam lifetime and losses (dynamic aperture) is clearly visible

- Number of head-on and/or long range interactions important for losses and all predicted PACMAN effects are observed

All observations are in good agreement with the expectations and an analytical model [11]. From this first experience we have confidence that beam-beam effects in the LHC are understood and should allow to reach the target luminosity for the nominal machine at 7 TeV beam energy. The analytical model [11] should allow to extrapolate the results to different configurations and allow an optimization of the relevant parameters.

## ACKNOWLEDGEMENTS

These studies would have been impossible without the help and support from the operations teams for the LHC and its injectors. We are also grateful to the LHC experiments for the collaboration during our studies and for providing us with luminosity and background data.

## REFERENCES

- [1] W. Herr, "Features and implications of different LHC crossing schemes", CERN LHC Project Report 628 (2003).
- [2] G. Papotti, "Observations of beam-beam effects in the LHC", These proceedings.
- [3] W. Herr, "Dynamic behaviour of nominal and PACMAN bunches for different LHC crossing schemes", CERN LHC Project Report 856 (2005).
- [4] W. Fischer, "Beam-beam compensation schemes", Session at this workshop.
- [5] T. Pieloni, "Beam-beam studies in the LHC and new projects", These proceedings.
- [6] G. Trad, "Beam-beam effects with a high pile-up test in the LHC", These proceedings.
- [7] W. Herr et al, "Head-on beam-beam interactions with high intensities and long range beam-beam studies in the LHC", CERN-ATS-Note-2011-058 (2011).
- [8] W. Herr, D. Kaltchev, "Results of dynamic aperture studies with increased  $\beta^*$  with beam-beam interactions", LHC Project Note 416 (2008).
- [9] W. Herr, D. Kaltchev et al, "Large Scale Beam-beam Simulations for the CERN LHC using distributed computing", Proc. EPAC 2006, Edinburgh (2006).
- [10] W. Herr, D. Kaltchev, "Analytical calculation of the smear for long range beam-beam interactions", IPAC 2009, Vancouver (2009).
- [11] D. Kaltchev, "Analysis of long range studies in the LHC - comparison with the model", These proceedings.
- [12] D. Neuffer and S. Peggs, "Beam-beam tune shifts and spreads in the SSC: head-on, long range, and PACMAN conditions", SSC Report, SSC-63 (1986).
- [13] W. Herr and H. Grote, "Self-consistent orbits with beam-beam effects in the LHC", Proc. 2001 Workshop on beam-beam effects, FNAL, 25.6.-27.6.2001, (2001).
- [14] W. Kozanecki and J. Cogan, private communication (2011).
- [15] R. Bartoldus, "Online determination of the LHC Luminous Region with the ATLAS High Level trigger", TIPP 2011, Int. Conf. on Tech. and Instr. in Particle Physics, Chicago (2011).